



KOH activated cattail-leaf-based carbon as an effective adsorbent for removal of methylene blue from aqueous solutions

Yao Li^{a,b}, Miao Yu^{a,b}, Jian Li^{a,b}, Lijuan Wang^{a,b,*}

^aKey Laboratory of Bio-based Materials Science and Technology of Ministry of Education, Northeast Forestry University, Harbin, China, Tel. 86-15561580982, email: 764408207@qq.com (Y. Li), Tel. 86-18804639130, email: 1217182027@qq.com (M. Yu), Tel. 86-451-82191693, email: nefulijian@163.com (J. Li), Tel. 86-451-82191693, email: donglinwlj@163.com (L. Wang)

^bResearch Center of Wood Intelligent Science, Northeast Forestry University, Harbin, China

Received 5 July 2018; Accepted 6 December 2018

ABSTRACT

In this paper, activated carbon was prepared from cattail leaves (C-AC) by two-step procedures using KOH as the activation agent. The structure and morphology of C-AC were characterized by scanning electron microscopy, nitrogen adsorption and X-ray diffraction. C-AC that was highly porous and had a high specific surface area ($1546.56 \text{ m}^2 \cdot \text{g}^{-1}$) were obtained under activation at 750°C for 40 min, which the adsorption process and equilibrium of methylene blue closely obeyed the pseudo-second-order kinetic model and Langmuir isotherm. The adsorption capacity reached $498.95 \text{ mg} \cdot \text{g}^{-1}$ with 15 mg adsorbent in $100 \text{ mg} \cdot \text{L}^{-1}$ for 30 min at 303.15 K. The adsorption was endothermic, spontaneous, and a physically controlled process. This work provides a potential adsorbent from cattail leaves for purification of wastewater containing dyes.

Keywords: Activated carbon; Cattail leaves; Methylene blue; Adsorption

1. Introduction

In various industries, dyes are used frequently and make life colorful. Improper discharge of wastewater will result in severe environmental problems. The toxicity and irritation of dyes can harm animals, plants and even human life [1–3]. Wastewater containing dyes must be purified before discharged. Compared to other methods, adsorption is a desirable way because of its simplicity in operation and process control, high efficiency, as well as low material and operational costs [4–6]. Activated carbon (AC) is an often-used adsorbent for effective removal of dyes from wastewater. As we all known that AC [7] is a carbon-rich material containing a well-built internal pore structure. The high surface area, well-organized macro-, meso-, and micropores, as well as a wide range of chemical functional groups on the surface of AC confer its versatile applications.

Biomass such as wood, nutshells, crops, crop waste, and animal dung is the most abundant organic renewable

resource in nature; it is inexpensive and has complicated structures. Biomass-based AC provides more choices for solving environmental problems. Methylene blue is cationic dye widely used in textile dyeing and as an additive for petroleum products. In a short period of time, it has harmful effects on organisms. AC from various biomass like fir wood, pine wood, oil palm wood, and apple shell showed adsorption capacities of 580.1, 556, 90.9, and $48.31 \text{ mg} \cdot \text{g}^{-1}$ for methylene blue, respectively [8]. AC from *Posidonia oceanica* leaves using ZnCl_2 as the activating agent showed an adsorption capacity of $285.7 \text{ mg} \cdot \text{g}^{-1}$ for methylene blue [9]. The alginate-beads-based AC had an adsorption capacity of up to $230 \text{ mg} \cdot \text{g}^{-1}$ for methylene blue [10]. AC that prepared from cashew nut shell obtained by ZnCl_2 activation could adsorb methylene blue up to $476 \text{ mg} \cdot \text{g}^{-1}$ [11]. The above works indicated that AC from raw material with different original structures exhibited different adsorption performance. Therefore, it is necessary to search for cheap and effective alternatives. Cattail [12] is a genus of about 30 species of monocotyledonous flowering plants. It thrives in shallow water with a depth of 1 m or more. Because aquatic plants have relatively devel-

*Corresponding author.

oped aeration tissues, all the organs of cattail used for nutrition have air cavities or ventilation tissues, which lead to a large number of holes. The leaf length of cattail is 54–120 cm, the upper part of which is flat and the lower part is a sponge-like structure that is suitable for forming AC. The Brunauer-Emmett-Teller surface areas of cattail-based AC by H_3PO_4 activation were $1279 \text{ m}^2\cdot\text{g}^{-1}$ and $1172 \text{ m}^2\cdot\text{g}^{-1}$ [13,14]. KOH activation is an often-used method to prepare activated carbon [15]. However, AC from cattail leaves prepared through KOH activation has not been reported so far.

In this study, AC was prepared from cattail leaves as starting material by using KOH as the activation agent, which was used for the purification of methylene blue from aqueous solutions.

2. Material and methods

2.1. Chemicals and raw materials

Potassium hydroxide (KOH), hydrochloric acid (HCl, 98%), NaOH and methylene blue were supplied by Yongda Chemical Reagent Company Limited (Tianjin, China). All of the chemicals were of analytical grade and were used as received. Cattail leaves were collected from Daqing, Heilongjiang Province.

2.2. Preparation of activated carbon

2.2.1. Carbonization process

The cattail leaves were cut into uniform pieces (1 cm × 1 cm) and then ground to form a powder using a grinder (Tianjin, China) and sieved to obtain particles with an 80–100 mesh.

Cattail leaf particles were placed in a porcelain boat and placed in the middle of a tubular resistance furnace. The first stage was performed from room temperature to 400°C at a heating rate of $10^\circ\text{C}\cdot\text{min}^{-1}$ for 40 min in a nitrogen atmosphere. The carbonized material was cooled to room temperature in a nitrogen atmosphere and then taken out for further activation.

2.2.2. Activation process

The carbonized material was immersed in KOH solution at 80°C for 16 h, dried in an oven at 105°C , and then

placed in a tubular furnace. The porcelain boat was heated to the specified temperature (Table 1) in a nitrogen atmosphere. The activated sample was then immersed in $0.01 \text{ mol}\cdot\text{L}^{-1}$ HCl for 10 h, washed with distilled water at 80°C until a neutral pH of the washings was achieved, and dried at 105°C for 20 h. The obtained products were denoted as C-AC-X-Y (X = 700, 750°C ; Y = 40, 50, 60 min).

2.3. Characterization of C-AC-X-Y

The surface morphologies of C-AC-X-Y were examined by using a scanning electron microscope (Hitachi SU-70, Japan). A thin layer of gold was sprayed on the surfaces of the samples before observation. C-AC-X-Y was characterized by the adsorption-desorption isotherm of nitrogen (ASAP 2020) at 77 K. The Brunauer-Emmet-Teller method was used to determine the specific surface area and the pore size distribution was calculated through the Barrett-Joyner-Halenda method. X-ray diffractometer (XRD) (Rigaku, D/max 2200) with Cu $K\alpha$ radiation was utilized to analyze the crystal structure of the samples.

2.4. Adsorption experiments

The experiments for batch adsorption were carried out in a water bath shaker. In each experiment, a certain dosage of C-AC-X-Y and 50 mL of methylene blue were mixed together in a conical flask and shaken at 110 rpm. The adsorbents were removed by centrifugation after adsorption, and the residual dye solution was obtained. The absorbance of the residual dye solution and the standard curves of the dye solution were recorded with a UV-visible spectrophotometer (7230 G). The effects of the dosage, temperature, initial pH value, concentration, and contact time were studied. The pH of the dye solutions was adjusted using $0.01 \text{ mol}\cdot\text{L}^{-1}$ HCl or NaOH solution. In this work, C-AC-750-40 was used to study the adsorption performance.

3. Results and discussion

3.1. Characterization of the prepared AC

3.1.1. SEM

The SEM images of cattail leaf, carbonized cattail leaf and C-AC-750-40 are shown in Fig. 1. As shown in Fig. 1a the

Table 1
Preparation scheme and results of AC from cattail leaf

Number	KOH:C	Carbonization	Carbonization	A	B	C	D
		Temperature ($^\circ\text{C}$)	Time (min)				
1	4:1	400	40	700	40	496.14	50.49
2				700	50	494.63	58.16
3				700	60	471.96	55.61
4				750	40	498.95	34.67
5				750	50	498.79	32.09
6				750	60	189.27	32.22

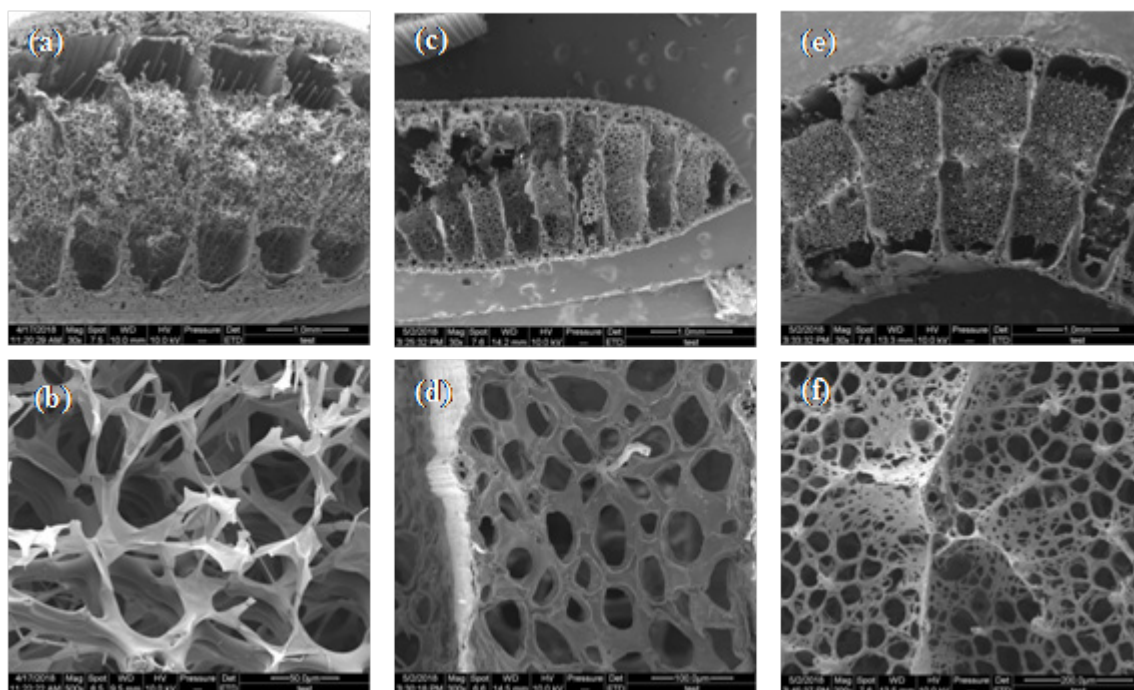


Fig. 1. SEM images of cattail leaf at (a) $\times 30$ and (b) $\times 500$; carbonized cattail leaf at (c) $\times 30$ and (d) $\times 300$; and C-AC-750-40 at (e) $\times 30$ and (f) $\times 200$. C-AC is the abbreviation of activated carbon prepared from cattail leaves; X denotes the activation temperature; Y presents the activation time. C-AC-700-50, C-AC-750-40 are the abbreviation of activated carbon prepared from cattail leaves activation at 700°C for 50min and 750°C for 40min, respectively.

interior of the cattail leaf, such as aerenchyma, vascular bundle, parenchyma cell, and posterior wall cell, has a complicated structure. The thickness of the leaf epidermis is around 0.5 mm. After carbonization, the leaf obviously shrunk and the thickness of the leaf epidermis decreased down to 50%. After activation, the main structure was similar to that of the carbonized cattail leaf. As shown in Figs. 1c and 1d, the 3D network of the cattail leaf is clearly visible, and carbonization causes the pore diameter to decrease and the pore wall to wrinkle after magnification. More new pores form on the wall, which become thinner after activation (Fig. 1e) resulting from the reaction between the carbon atoms and KOH under high temperature in the activation process.

3.1.2. BET

According to the Brunauer–Emmet–Teller and Barrett–Joyner–Halenda methods, the specific surface area and pore size distribution of C-AC-X-Y samples were studied by using N_2 adsorption/desorption experiments. As shown in Fig. 2a, C-AC-X-Y has a typical type IV adsorption/desorption isotherm according to the IUPAC classification. The platform is close to horizontal, suggesting that there are a large number of microporous structures in AC. The N_2 adsorption isotherm for each sample rapidly increases and the adsorption rate is rapid in the relative pressure range (P/P_0) of <0.1 , indicating the existence of micropores [16]. When the relative pressure is in the range of $0.1 < P/P_0 < 1$, the nitrogen isotherm tends to rise slowly, showing that AC in the relatively high-pressure area of N_2 adsorption quantity is very scant. There is a closed loop in the stripping absorption curve. The adsorption

branches do not overlap [17]. As shown in Table 2, higher temperature and longer time are beneficial to the formation of pore structure. The C-AC-750-40 is highly porous and has a high specific surface area ($1546.56 \text{ m}^2\text{-g}^{-1}$) and average pore size of 2.1704 nm.

3.1.3. XRD

From the XRD diagram, two broad diffraction peaks appeared at about 23° and 43° , which can be indexed to the (002) and (100) lattice planes [18], indicating the characteristic of amorphous carbon of AC. High intensity in the low angle region may be due to large ratio of micropores in the six samples which is further confirmed from the N_2 adsorption-desorption measurements in Figs. 2a and 2b. As shown in Fig. 2c, the diffraction peak intensity of sample C-AC-750-40 is the lowest which certifies that its crystallinity is the lowest, the ordered structure of the molecule is the most disruptive, and there are more holes and gaps between molecules. Therefore, methylene blue is easier to enter the inside of C-AC-750-40. This proves that the adsorption capacity of C-AC-750-40 is the largest in all samples.

3.2. Performance in methylene blue adsorption

3.2.1. Effect of dosage of C-AC-750-40 on the adsorption

The effect of the AC dosage on the removal rate of methylene blue is shown in Fig. 3a. When the AC dose increased from 5 mg to 30 mg, the removal rate increased from 92.7% to 99.98% and the absorption capacity increased from 315.6

Table 2
Pore structural parameters and specific capacity of the C-AC-X-Y samples

Sample	S_{BET} $\text{m}^2\cdot\text{g}^{-1}$	S_{Langmuir} $\text{m}^2\cdot\text{g}^{-1}$	$S_{\text{Micropore}}$ $\text{m}^2\cdot\text{g}^{-1}$	V_{Total} $\text{cm}^3\cdot\text{g}^{-1}$	$V_{\text{Micropore}}$ $\text{cm}^3\cdot\text{g}^{-1}$	D nm
C-AC-700-40	1245.06	1826.27	1080.74	0.6479	0.5649	2.0815
C-AC-700-50	1421.13	2093.72	931.93	0.7587	0.4955	2.1489
C-AC-700-60	984.54	1442.07	871.51	0.5016	0.4553	2.0379
C-AC-750-40	1546.56	2273.26	1255.86	0.8392	0.6565	2.1704
C-AC-750-50	1283.69	1900.22	901.93	0.6703	0.4798	2.0888
C-AC-750-60	565.15	831.65	468.15	0.3145	0.2445	2.2262

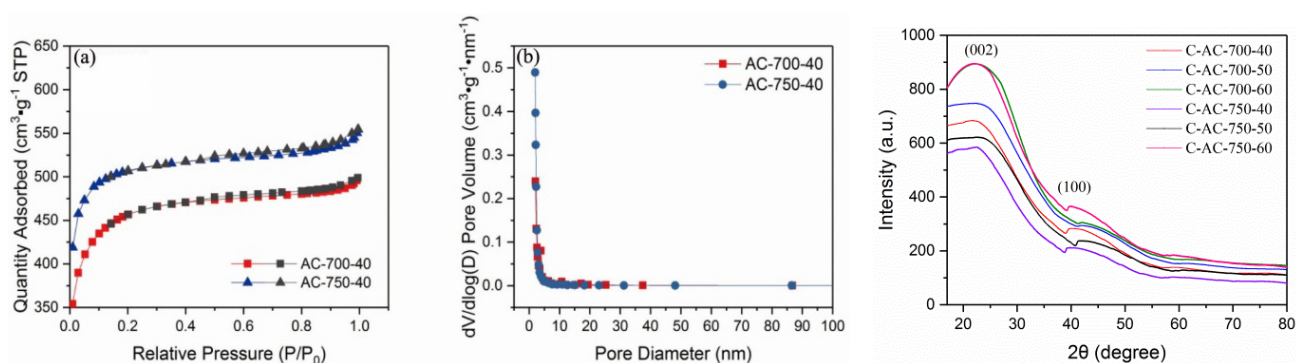


Fig. 2 (a) N_2 adsorption–desorption isotherms of C-AC-700-50 and C-AC-750-40; (b) BJH pore-size distributions (inset) of C-AC-700-50 and C-AC-750-40; (c) XRD patterns of the C-AC-X-Y samples. C-AC is the abbreviation of activated carbon prepared from cattail leaves; X denotes the activation temperature; Y presents the activation time. C-AC-700-50 and C-AC-750-40 are the abbreviation of activated carbon prepared from cattail leaves activation at 700°C for 50 min and 750°C for 40 min, respectively.

$\text{mg}\cdot\text{g}^{-1}$ to 498.95 $\text{mg}\cdot\text{g}^{-1}$. This phenomenon is due to the increase in adsorbent dosage, which provides more active adsorption sites and increases the contact area of the dye and adsorbent so that the removal rate increases. When the adsorbent was more than 10 mg, the change in removal rate was not obvious, and the dye solution was colorless. C-AC-750-40 was therefore effective for the removal of methylene blue from aqueous solution.

3.2.2. Effect of pH on the adsorption

The effect of pH on the removal rate of methylene blue is shown in Fig. 3b. The pH affects not only the surface charge of the adsorbent, but also the chemical properties of the dye solution [19]. The effect of pH on the adsorption of methylene blue by C-AC-750-40 was not significant, about 99.8–99.85%. Therefore, the pH in the experimental range has little effect on the adsorption of methylene blue on C-AC-750-40. The reason is that the adsorption of the dye group is first affected by the surface charge of the AC, and is then affected by the pH of the solution. The surface of the polar functional group provides a sufficient negative charge, which gives AC a better adsorption effect for methylene blue.

3.2.3. Effect of initial dye concentration on the adsorption

The effect of the initial dye concentration on the removal rate of methylene blue is shown in Fig. 3c. As the initial

concentration of methylene blue increased, the removal rate decreased gradually from 99.99% to 63.35%. Because of the constant adsorbent dosage, the adsorption sites were also certain. When the adsorption reached equilibrium, the adsorption sites were saturated. When the initial concentration of methylene blue increased, the removal rate decreased. The increase in methylene blue concentration increased the probability of collision with the adsorbent and increased the adsorption capacity. Because of the restriction of adsorption capacity, however, the adsorption capacity of C-AC-750-40 for methylene blue decreased gradually.

3.2.4. Effect of contact time on the adsorption

The adsorption dynamics of the methylene blue system strongly depend on the contact time. As shown in Fig. 3d, the change in adsorption capacity during the first 60 min took place the fastest and then became slower. The equilibrium time of the adsorption of methylene blue on C-AC-750-40 at 303.15 K was 120 min, and the corresponding adsorption capacity was 498.95 $\text{mg}\cdot\text{g}^{-1}$. At the beginning of adsorption, methylene blue is mainly adsorbed on the surface of C-AC-750-40, resulting in a high adsorption rate. With the adsorption process, the methylene blue concentration gradually decreased. At the same time, methylene blue diffused into the pores of C-AC-750-40 and the diffusion resistance gradually increased. The adsorption rate is mainly dependent on the diffusion rate, resulting in a

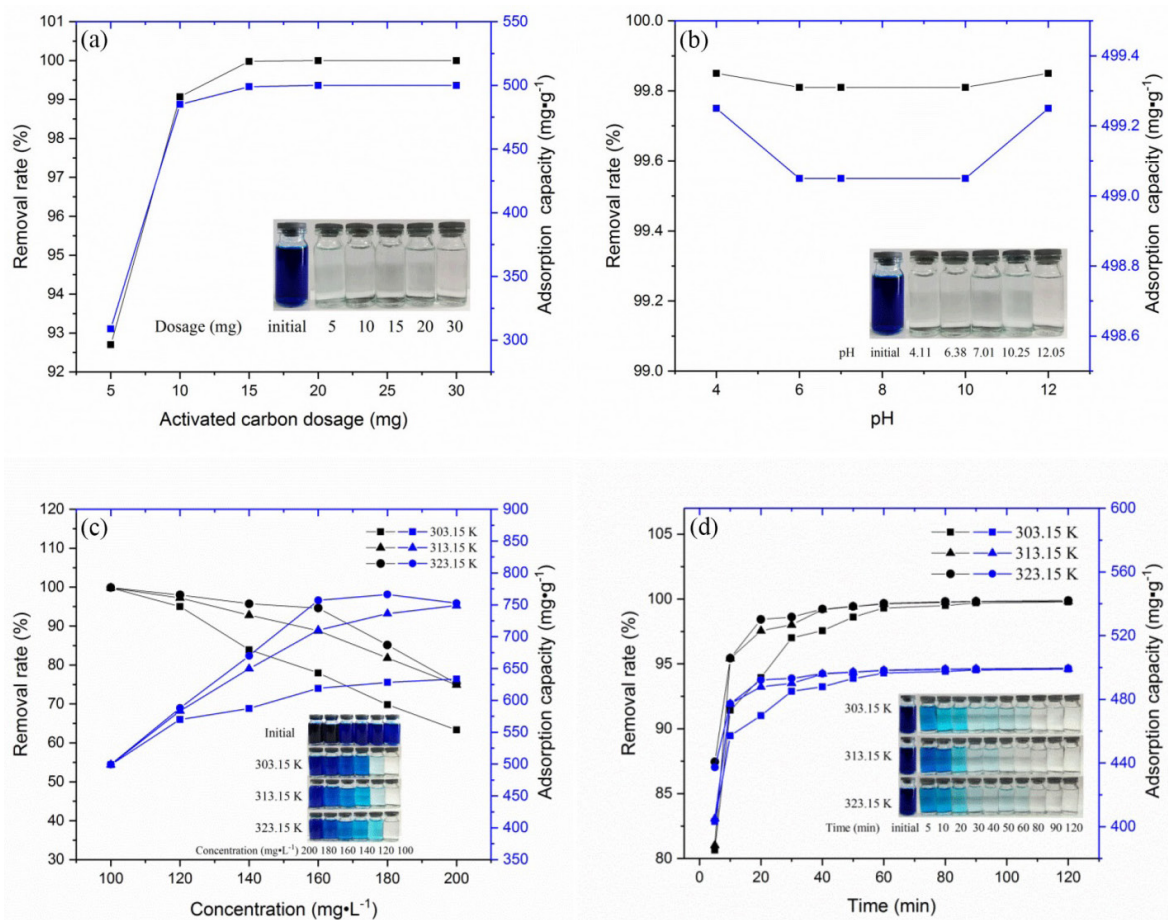


Fig. 3. The effect of (a) activated carbon dosage ($T = 303.15\text{ K}$; $t = 5\text{ h}$; $C = 100\text{ mg}\cdot\text{L}^{-1}$; $V = 50\text{ mL}$), (b) pH (dosage = 10 mg ; $T = 303.15\text{ K}$; $t = 2\text{ h}$; $C = 100\text{ mg}\cdot\text{L}^{-1}$; $V = 50\text{ mL}$), (c) concentration (dosage = 10 mg ; $t = 2\text{ h}$; $V = 50\text{ mL}$), and (d) contact time (dosage = 10 mg ; $C = 100\text{ mg}\cdot\text{L}^{-1}$; $V = 50\text{ mL}$) on the adsorption of methylene blue.

lower adsorption rate. At the end of adsorption, adsorption mainly occurs in the pore surface of AC. The driving force weakens, and adsorption reaches equilibrium. The removal rate changes from 80.65% to 99.89%.

3.3. Adsorption isotherms

Langmuir [20] and Freundlich [21] isotherm models are well-known adsorption isotherms. The equilibrium adsorption of methylene blue on C-AC-750-40 at 303.15 K, 313.15 K, and 323.15 K was analyzed using adsorption isotherms, as discussed below (Table 3). The R^2 values of the Langmuir isotherms are 0.99956, 0.99922, and 0.99954, respectively. However, R^2 values of the Freundlich isotherms are much lower. These indicate that the data fitted well the Langmuir isotherm in the present adsorption studies.

3.4. Adsorption kinetic models

In this study, three kinetic models were used to describe the reaction order of adsorption of C-AC-750-40 on methylene blue, such as the pseudo-first-order model [22], pseudo-second-order model [23,24], and intraparticle diffusion

Table 3

The parameters of adsorption isotherms for methylene blue at different temperatures

	T (K)		
	303.15	313.15	323.15
Langmuir			
$K_L, \text{L}\cdot\text{mg}^{-1}$	1.223	1.078	2.966
$q_m, \text{mg}\cdot\text{g}^{-1}$	636.968	758.081	761.215
R^2	0.99956	0.99922	0.99954
Freundlich			
$K_F, \text{L}\cdot\text{g}^{-1}$	530.033	556.524	587.103
$1/n$	0.04043	0.07559	0.07558
R^2	0.98208	0.97089	0.89922

model [25]. Fig. 3d shows that equilibrium was established at 60 min at a temperature of 303.15 K, while equilibrium was reached at 50 min at 313.15 K and 323.15 K. The corresponding adsorption capacities were $498.95\text{ mg}\cdot\text{g}^{-1}$, $499.10\text{ mg}\cdot\text{g}^{-1}$, and $499.45\text{ mg}\cdot\text{g}^{-1}$.

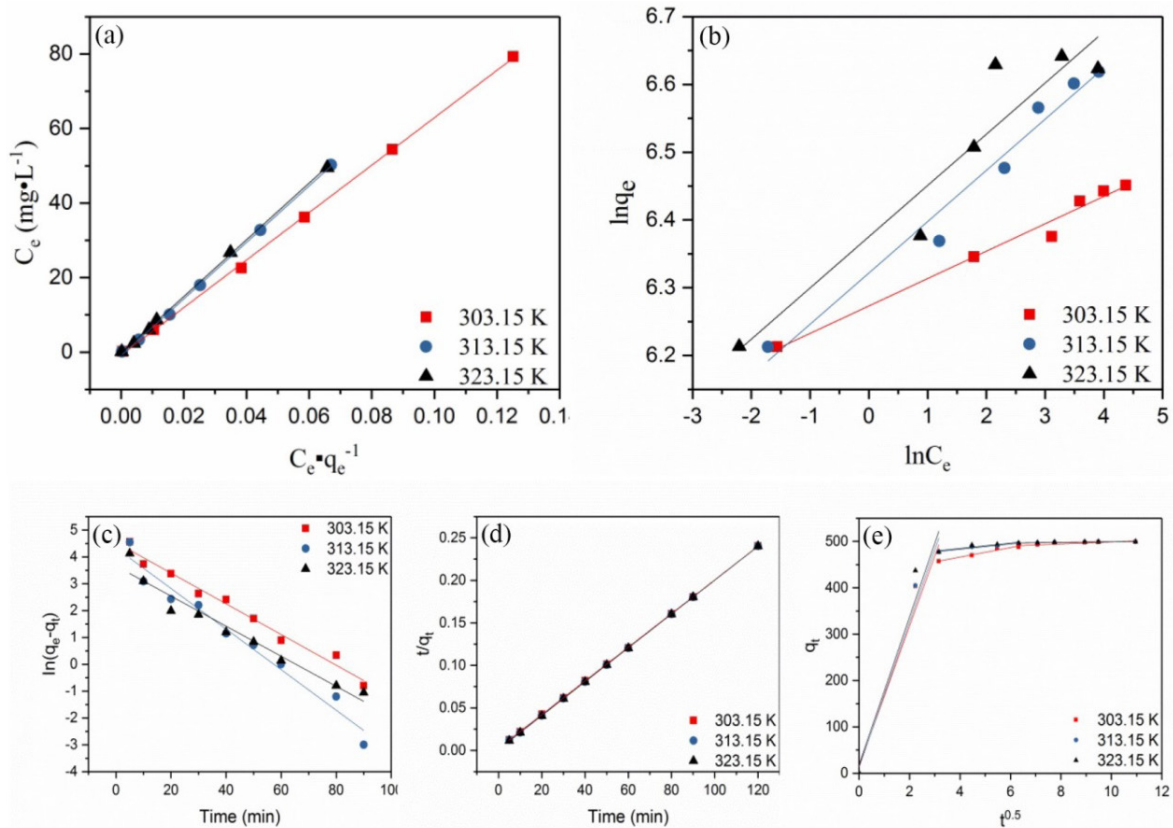


Fig. 4. Fitting curves of the (a) Langmuir isotherm, (b) Freundlich isotherm, (c) pseudo-first-order model and (d) pseudo-second-order model; (e) intraparticle diffusion equation.

The plots and parameters of kinetic model for C-AC-740-40 are shown in Figs. 4c, d, e and Table 4. The correlation coefficients R^2 (~0.99) of the pseudo-second-order model were more uniform and higher than those of the pseudo-first-order model. Moreover, the calculated adsorption capacity ($q_{e,cal}$) from the pseudo-second-order model was closer to the experimental adsorption capacity ($q_{e,exp}$). As the temperature increased, K_2 gradually became larger. This indicates that the increased temperature was favorable for the adsorption. The results suggested that the adsorption of methylene blue on C-AC-750-40 fitted the pseudo-second-order model better than the pseudo-first-order model.

The plot in Fig. 4e is not linear over the entire time range. In three consecutive processes, the adsorption of methylene blue on C-AC-750-40 is continuous. This behavior suggests that more than one process affects adsorption, but only one process limits the rate within a specific time frame. In the initial stage of adsorption reaction, a good linear relationship was shown. This process corresponds to the diffusion of dye molecules from the solution body to the adsorbent surface. The second part corresponds to the slow adsorption process, in which the internal diffusion is the decisive step. The third part is adsorption equilibrium. The slope of the linear portion reflects the rate of adsorption.

The Arrhenius equation [26] was used to calculate the activation energy of the adsorption:

$$\ln K_2 = -E_a/RT + \ln K_0$$

Table 4

The parameters of kinetic models for methylene blue adsorption at different temperatures

	T (K)		
	303.15	313.15	323.15
$q_{e,exp}$, mg·g ⁻¹	498.95	499.10	499.45
Pseudo-first-order			
K_1 , min ⁻¹	0.05720	0.07555	0.05601
$q_{e,cal}$, mg·g ⁻¹	93.86	76.32	38.92
R^2	0.98185	0.96711	0.95442
Pseudo-second-order			
$K_2 \times 10^3$, mg·g ⁻¹ ·min ⁻¹	1.62	2.75	3.77
$q_{e,cal}$, mg·g ⁻¹	505.05	502.50	502.50
R^2	0.99998	0.99997	0.99999
Intraparticle diffusion			
k_{i1} , mg·g ⁻¹ ·min ^{-0.5}	151.1712	156.4675	159.1489
R^2	0.96767	0.97813	0.95517
k_{i2} , mg·g ⁻¹ ·min ^{-0.5}	10.31003	5.66515	5.72376
R^2	0.96619	0.95937	0.84542
k_{i3} , mg·g ⁻¹ ·min ^{-0.5}	2.19192	0.67837	0.70286
R^2	0.76288	0.82722	0.86030

The value of E_a is also evaluated by plotting $\ln K_2$ versus T^{-1} . Generally speaking, low activation energies (5–40 $\text{kJ}\cdot\text{mol}^{-1}$) are characteristic of physical adsorption. In this study, the E_a value is $34.48 \text{ kJ}\cdot\text{mol}^{-1}$ for the adsorption of methylene blue on C-AC-750-40. It is shown that the adsorption should be a physically controlled process.

3.5. Thermodynamic parameters

It is important to study the thermodynamic parameters for evaluating the spontaneity of the adsorption process. The adsorption of methylene blue by C-AC-750-40 was calculated from temperature data and the free energy change (ΔG°), enthalpy change (ΔH°), and entropy change (ΔS°) [27,28]:

The values of ΔG° and ΔH° were obtained from the slope and intercept of the van't Hoff curve. The thermodynamic parameters are as follows: $\Delta H^\circ = 150.628 \text{ kJ}\cdot\text{mol}^{-1}$, $\Delta S^\circ = 26.218 \text{ J}\cdot\text{K}^{-1}\cdot\text{mol}^{-1}$ and $\Delta G^\circ = -19.591 \text{ kJ}\cdot\text{mol}^{-1}$, $-20.640 \text{ kJ}\cdot\text{mol}^{-1}$, $-22.624 \text{ kJ}\cdot\text{mol}^{-1}$ at 303.15 K, 313.15 K, and 323.15 K, respectively. The negative value of ΔG° [29] reflects the spontaneous and viable adsorption of methylene blue on the adsorbent. ΔH° has a positive value [30], indicating that the adsorption is endothermic. ΔS° has a positive value [31], which shows that the randomness of the interface increases during the adsorption process. These results prove that the higher the temperature, the better the adsorption effect.

4. Conclusions

In summary, AC was prepared by two-step procedures with single KOH as the activation agent from cattail leaves. SEM showed that cattail leaf had complex internal structures. Carbonization made the pore diameter decrease and the pore wall wrinkle. After activation, C-AC-750-40 exhibited high specific surface areas ($1546.56 \text{ m}^2\cdot\text{g}^{-1}$) and an average pore size of 2.1704 nm. The maximum adsorption capacity for methylene blue at equilibrium was $498.95 \text{ mg}\cdot\text{g}^{-1}$. The adsorption followed the Langmuir isotherm and the pseudo-second-order kinetic well. The calculated activation energy is $34.48 \text{ kJ}\cdot\text{mol}^{-1}$, indicating that the adsorption of methylene blue onto activated carbon is a physically controlled process. Adsorption is a spontaneous and endothermic process, as thermodynamic studies have shown. This research indicates that C-AC is a promising adsorbent for purification of wastewater.

Acknowledgements

This work was supported by the Fundamental Research Funds for Central Universities (E2572017EB05) and Heilongjiang Province outstanding youth science fund (JC201301).

References

- [1] T.N.V. de Souza, S.M.L. de Carvalho, M.G.A. Vieira, M.G.C. da Silva, D.d.S.B. Brasil, Adsorption of basic dyes onto activated carbon: Experimental and theoretical investigation of chemical reactivity of basic dyes using DFT-based descriptors, *Appl. Surf. Sci.*, 448 (2018) 662–670.
- [2] M. Goswami, P. Phukan, Enhanced adsorption of cationic dyes using sulfonic acid modified activated carbon, *J. Environ. Chem. Eng.*, 5 (2017) 3508–3517.
- [3] S. Wong, N.A.N. Yac'cob, N. Ngadi, O. Hassan, I.M. Inuwa, From pollutant to solution of wastewater pollution: Synthesis of activated carbon from textile sludge for dye adsorption, *Chin. J. Chem. Eng.*, 26 (2018) 870–878.
- [4] P. Lodha, A.N. Netravali, Characterization of stearic acid modified soy protein isolate resin and ramie fiber reinforced 'green' composites, *Compos. Sci. Technol.*, 65 (2005) 1211–1225.
- [5] J. Anandkumar, B. Mandal, Adsorption of chromium(VI) and Rhodamine B by surface modified tannery waste: kinetic, mechanistic and thermodynamic studies, *J. Hazard. Mater.*, 186 (2011) 1088–1096.
- [6] K. Shakir, A.F. Elkafrawy, H.F. Ghoneimy, S.G. Elrab Beheir, M. Refaat, Removal of rhodamine B (a basic dye) and thoron (an acidic dye) from dilute aqueous solutions and wastewater simulants by ion flotation, *Water Res.*, 44 (2010) 1449–1461.
- [7] J. Kazmierczak-Razna, P. Nowicki, M. Wiśniewska, A. Nosal-Wiercińska, R. Pietrzak, Thermal and physicochemical properties of phosphorus-containing activated carbons obtained from biomass, *J. Taiwan Inst. Chem. E.*, 80 (2017) 1006–1013.
- [8] M. Danish, T. Ahmad, A review on utilization of wood biomass as a sustainable precursor for activated carbon production and application, *Renew. Sustain. Energy Rev.*, 87 (2018) 1–21.
- [9] M.U. Dural, L. Cavas, S.K. Papageorgiou, F.K. Katsaros, Methylene blue adsorption on activated carbon prepared from *Posidonia oceanica* (L.) dead leaves: Kinetics and equilibrium studies, *Chem. Eng. J.*, 168 (2011) 77–85.
- [10] A. Nasrullah, A.H. Bhat, A. Naeem, M.H. Isa, M. Danish, High surface area mesoporous activated carbon-alginate beads for efficient removal of methylene blue, *Int. J. Biol. Macromol.*, 107 (2018) 1792–1799.
- [11] A.A. Spagnoli, D.A. Giannakoudakis, S. Bashkova, Adsorption of methylene blue on cashew nut shell based carbons activated with zinc chloride: The role of surface and structural parameters, *J. Mol. Liq.*, 229 (2017) 465–471.
- [12] Q.M. Rahman, L. Wang, B. Zhang, S. Xiu, A. Shahbazi, Green biorefinery of fresh cattail for microalgal culture and ethanol production, *Bioresour. Technol.*, 185 (2015) 436–440.
- [13] Q. Shi, J. Zhang, C. Zhang, C. Li, B. Zhang, W. Hu, J. Xu, R. Zhao, Preparation of activated carbon from cattail and its application for dyes removal, *J. Environ. Sci.*, 22 (2010) 91–97.
- [14] J. Zhang, Q. Shi, C. Zhang, J. Xu, B. Zhai, B. Zhang, Adsorption of Neutral Red onto Mn-impregnated activated carbons prepared from *Typha orientalis*, *Bioresour. Technol.*, 99 (2008) 8974–8980.
- [15] J.M. Salman, V.O. Njoku, B.H. Hameed, Bentazon and carbofuran adsorption onto date seed activated carbon: Kinetics and equilibrium, *Chem. Eng. J.*, 173 (2011) 361–368.
- [16] H. Wang, T. Zhu, X. Fan, H. Na, Adsorption and desorption of small molecule volatile organic compounds over carbide-derived carbon, *Carbon*, 67 (2014) 712–720.
- [17] W.H. Qu, Y.Y. Xu, A.H. Lu, X.Q. Zhang, W.C. Li, Converting biowaste corncob residue into high value added porous carbon for supercapacitor electrodes, *Bioresour. Technol.*, 189 (2015) 285–291.
- [18] F. Tao, Y.Q. Zhao, G.Q. Zhang, H.L. Li, Electrochemical characterization on cobalt sulfide for electrochemical supercapacitors, *Electrochem. Commun.*, 9 (2007) 1282–1287.
- [19] G. Crini, P.-M. Badot, Application of chitosan, a natural aminopolysaccharide, for dye removal from aqueous solutions by adsorption processes using batch studies: A review of recent literature, *Prog. Polym. Sci.*, 33 (2008) 399–447.
- [20] C. Namasivayam, D. Kavitha, Removal of Congo Red from water by adsorption onto activated carbon prepared from coir pith, an agricultural solid waste, *Dyes Pigm.*, 54 (2002) 47–58.
- [21] A. Altinisik, E. Gur, Y. Seki, A natural sorbent, *Luffa cylindrica* for the removal of a model basic dye, *J. Hazard. Mater.*, 179 (2010) 658–664.
- [22] Y.S. Ho, G. McKay, Kinetic models for the sorption of dye from aqueous solution by wood, *Process Saf. Environ. Prot.*, 76 (1998) 183–191.

- [23] Y.S. Ho, G. McKay, Pseudo-second order model for sorption processes, *Process Biochem.*, 34 (1999) 451–465.
- [24] B.H. Hameed, A.L. Ahmad, K.N.A. Latiff, Adsorption of basic dye (methylene blue) onto activated carbon prepared from rat-tan sawdust, *Dyes Pigm.*, 75 (2007) 143–149.
- [25] B.H. Hameed, I.A.W. Tan, A.L. Ahmad, Adsorption isotherm, kinetic modeling and mechanism of 2,4,6-trichlorophenol on coconut husk-based activated carbon, *Chem. Eng. J.*, 144 (2008) 235–244.
- [26] Q. Ma, L. Wang, Adsorption of Reactive blue 21 onto functionalized cellulose under ultrasonic pretreatment: Kinetic and equilibrium study, *J. Taiwan Inst. Chem. Eng.*, 50 (2015) 229–235.
- [27] N. Buvanewari, C. Kannan, Plant toxic and non-toxic nature of organic dyes through adsorption mechanism on cellulose surface, *J. Hazard. Mater.*, 189 (2011) 294–300.
- [28] Z. Aksu, Determination of the equilibrium, kinetic and thermodynamic parameters of the batch biosorption of nickel(II) ions onto *Chlorella vulgaris*, *Process Biochem.*, 38 (2002) 89–99.
- [29] L. Mouni, L. Belkhiri, J.-C. Bollinger, A. Bouzaza, A. Assadi, A. Tirri, F. Dahmoune, K. Madani, H. Remini, Removal of Methylene Blue from aqueous solutions by adsorption on Kaolin: Kinetic and equilibrium studies, *Appl. Clay Sci.*, 153 (2018) 38–45.
- [30] E.C. Peres, J.C. Slaviero, A.M. Cunha, A. Hosseini-Bandeghar-aei, G.L. Dotto, Microwave synthesis of silica nanoparticles and its application for methylene blue adsorption, *J. Environ. Chem. Eng.*, 6 (2018) 649–659.
- [31] O.O. Namal, E. Kalipci, Adsorption kinetics of methylene blue using alkali and microwave modified apricot stones, *J. Environ. Chem. Eng.*, (2017).